

Published in final edited form as:

Dev Cell. 2014 August 11; 30(3): 295–308. doi:10.1016/j.devcel.2014.06.005.

Integrin $\alpha\beta3$ Drives Slug Activation and Stemness in the Pregnant and Neoplastic Mammary Gland

Jay S Desgrosellier^{1,*}, Jacqueline Lesperance¹, Laetitia Seguin¹, Maricel Gozo¹, Shumei Kato², Aleksandra Franovic¹, Mayra Yebra¹, Sanford J Shattil², and David A Cheresch¹

¹Department of Pathology, Moores UCSD Cancer Center, University of California, San Diego, La Jolla, CA 92093, USA

²Division of Hematology-Oncology, Department of Medicine, University of California, San Diego, La Jolla, CA 92093, USA

SUMMARY

While integrin $\alpha\beta3$ expression is linked to breast cancer progression its role in epithelial development is unclear. Here, we show that $\alpha\beta3$ plays a critical role in adult mammary stem cells (MaSCs) during pregnancy. Whereas $\alpha\beta3$ is a luminal progenitor marker in the virgin gland, we noted increased $\alpha\beta3$ expression in MaSCs at mid-pregnancy. Accordingly, mice lacking $\alpha\beta3$ or expressing a signaling deficient receptor showed defective mammary gland morphogenesis during pregnancy. This was associated with decreased MaSC expansion, clonogenicity and expression of Slug, a master regulator of MaSCs. Surprisingly, $\alpha\beta3$ deficient mice displayed normal development of the virgin gland with no effect on luminal progenitors. TGF β 2 induced $\alpha\beta3$ expression leading to Slug nuclear accumulation and MaSC clonogenicity. In human breast cancer cells $\alpha\beta3$ was necessary and sufficient for Slug activation, tumorsphere formation and tumor initiation. Thus, pregnancy-associated MaSCs require a TGF β 2/ $\alpha\beta3$ /Slug pathway, which may contribute to breast cancer progression and stemness.

INTRODUCTION

In the adult mammary gland an epithelial hierarchy has been characterized that involves the step-wise differentiation of mammary stem cells (MaSC)/progenitor cells toward mature luminal and basal/myoepithelial cell fates (Visvader, 2009). MaSC/progenitor cells share a number of biological and biochemical properties with highly invasive breast cancer cells (Visvader, 2009) and thus may act as the cells-of-origin for more aggressive types of breast

© 2014 Elsevier Inc. All rights reserved.

*Correspondence should be addressed to: jdesgrosellier@ucsd.edu.

Publisher's Disclaimer: This is a PDF file of an unedited manuscript that has been accepted for publication. As a service to our customers we are providing this early version of the manuscript. The manuscript will undergo copyediting, typesetting, and review of the resulting proof before it is published in its final citable form. Please note that during the production process errors may be discovered which could affect the content, and all legal disclaimers that apply to the journal pertain.

AUTHOR CONTRIBUTIONS

J.S.D designed the project, performed experiments, analyzed the data and wrote the manuscript. J.L., L.S., M.G., S.K., A.F., and M.Y. helped design and conduct experiments and analyze data. S.J.S. provided help and expertise related to the $\beta3$ C mouse experiments. D.A.C. analyzed the data, supervised the overall project and wrote the manuscript.

cancer (Jeselson et al., 2010; Lim et al., 2009). Molecular profiling of mammary cells at distinct stages of differentiation identified gene signatures associated with particular MaSC and progenitor cells (Lim et al., 2010; Pece et al., 2010). The MaSC gene expression signature, in particular, correlates with tumors that are less differentiated (Lim et al., 2010) and represent clinically advanced disease (Pece et al., 2010). In some breast cancers, a subset of tumor cells has been identified that share similar gene expression (Pece et al., 2010) and behavioral properties (Al-Hajj et al., 2003) with normal MaSCs, and are referred to as cancer stem cells (CSCs).

Integrins act as key cell surface receptors regulating adhesion-dependent functions critical for MaSC/progenitor behavior (Taddei et al., 2008) and breast carcinogenesis (Desgrosellier and Cheresch, 2010). Integrin $\alpha v \beta 3$, in particular, is expressed in some of the most highly malignant tumor cells in carcinomas of the breast, pancreas, lung and prostate (Desgrosellier and Cheresch, 2010) where it may play an anchorage-independent role in tumor progression (Desgrosellier et al., 2009). Expression of $\beta 3$ (CD61) in breast carcinoma cells promotes both lymph node (Desgrosellier et al., 2009) and bone metastases (Felding-Habermann et al., 2001; Liapis et al., 1996; Sloan et al., 2006; Takayama et al., 2005) and serves as a marker of CSCs in some murine breast cancer models (Vaillant et al., 2008). In the normal murine mammary gland surface $\beta 3$ represents a marker of luminal progenitor cells (Asselin-Labat et al., 2007) and may be expressed on MaSCs (Bai and Rohrschneider, 2010), particularly in response to steroid hormones (Joshi et al., 2010). This suggests that $\alpha v \beta 3$'s function in carcinoma cells may be related to a role in normal MaSC/progenitor cell behavior.

The epithelial hierarchy in the adult mammary gland represents a well-characterized system with rigorously defined markers (Asselin-Labat et al., 2007; Shackleton et al., 2006; Stingl et al., 2006) allowing us to characterize a possible role for $\alpha v \beta 3$ in this process. Here we describe a role for $\alpha v \beta 3$ in regulating Slug activation in MaSCs leading to MaSC expansion and mammary gland remodeling during pregnancy. Interestingly, $\alpha v \beta 3$ also promotes Slug activation, anchorage-independent growth and tumor initiation in human breast cancer cells, hallmarks of tumor stemness.

RESULTS

$\beta 3$ is required for mammary gland development during pregnancy

Previous studies showed $\beta 3$ surface expression in luminal progenitors and some MaSCs from dissociated virgin mammary glands (Asselin-Labat et al., 2007). Consistent with these findings, we observed $\beta 3$ expression in basal cells and a subset of luminal cells within the ducts of adult virgin mice (Figure 1A) that was confirmed by co-staining with basal and luminal markers (Figure S1A). These results show that the $\beta 3$ expression pattern in the intact adult mammary gland is consistent with a potential role for $\beta 3$ in luminal progenitors and MaSCs.

The adult murine mammary gland is a highly dynamic organ, constantly changing in response to hormones released during the estrus cycle and pregnancy. Analysis of $\beta 3$ in whole-mammary gland lysates showed no differences during the estrus cycle (Figure S1B);

however, relative to virgin glands, we observed increased $\beta 3$ expression during early and mid-pregnancy that declined by late pregnancy (Figure 1B). Notably, the peak levels of $\beta 3$ at pregnancy day 12.5 (P12.5) coincide with the maximum number of MaSCs reported during pregnancy (Asselin-Labat et al., 2010).

$\beta 3$ expression in glands from both virgin and pregnant mice suggests a potential function for this receptor in mammary gland morphogenesis at either stage. To address this possibility, we examined the morphology of mammary gland whole-mounts from virgin and P12.5 wild-type (WT) and $\beta 3$ knock-out ($\beta 3$ KO) mice, which lack $\beta 3$ expression in the mammary gland (Figure S1C). While no differences were observed in mammary glands from virgin $\beta 3$ KO mice (Figure 1C; left panels), marked differences were seen in $\beta 3$ KO mammary glands at P12.5 which demonstrated fewer fine branches and alveolar buds relative to WT glands (Figure 1C; right panels). Importantly, this defect was maintained throughout late-stage pregnancy and lactation (Figure S1D,E) and correlated with decreased viability of litters born to $\beta 3$ KO dams (Figure S1F). However, we noted no difference in the ability of $\beta 3$ KO alveoli to produce milk at any stage examined (Figure S2A). Quantification of duct/alveoli density in H&E-stained sections showed a nearly 40% decrease in the density of P12.5 $\beta 3$ KO glands relative to WT controls (Figure 1D,E), consistent with the qualitative assessment of these glands. Thus, $\beta 3$ appears to be required for mammary development during pregnancy but not for ductal morphogenesis in the virgin adult gland.

To discern a potential mechanism that accounts for this phenotype, we assessed the relative amounts of epithelial cell proliferation, apoptosis and differentiation in WT and $\beta 3$ KO P12.5 mammary glands. Quantitative RT-PCR from whole mammary glands showed reduced mRNA levels of the alveolar marker *ELF5* (57% decrease), but not the luminal differentiation marker *GATA3* in P12.5 $\beta 3$ KO mammary glands relative to WT controls (Figure 1F). In contrast, we were unable to detect any effect on proliferation (Figure S2B,C) or apoptosis, which was essentially absent from the P12.5 gland (data not shown). Importantly, we noted similar levels of nuclear ELF5 protein in $\beta 3$ KO alveoli compared to those from WT mice (Figure S2D), indicating that the decreased ELF5 mRNA levels observed in P12.5 $\beta 3$ KO mammary glands is consistent with fewer alveoli and not due to dysregulated ELF5 expression. Taken together, these data show that $\beta 3$ deletion is associated with defective initiation of alveologenesis during pregnancy, suggesting that $\beta 3$ KO mice may display a defect in MaSC/progenitor cells.

Pregnancy is associated with increased $\beta 3$ expression in MaSCs

Mammary gland remodeling and differentiation during pregnancy requires the coordinated response of multiple cell types including MaSCs and progenitors (Asselin-Labat et al., 2010; Jeselsohn et al., 2010; van Amerongen et al., 2012; Van Keymeulen et al., 2011). To determine which MaSC/progenitor cell types might require $\beta 3$ during pregnancy we first compared $\beta 3$ expression in WT virgin and P12.5 mammary glands by flow cytometry. Analysis of live (propidium iodide negative) lineage negative (Lin^- ; CD31^- , CD45^- , Ter19^-) mammary cells for surface expression of CD24 and CD29 ($\beta 1$ integrin) identify enriched populations of mature luminal and progenitor cells ($\text{CD24}^+\text{CD29}^{\text{lo}}$) as well as basal and MaSCs ($\text{CD24}^+\text{CD29}^{\text{hi}}$) in both virgin (Shackleton et al., 2006) and P12.5 mammary

glands (Asselin-Labat et al., 2010). We then evaluated surface $\beta 3$ levels in these live $\text{Lin}^- \text{CD24}^+ \text{CD29}^{\text{hi/lo}}$ cells to determine the MaSC/progenitor cells that express $\beta 3$ during pregnancy. We found that most $\beta 3^+$ cells in the virgin gland resided in the CD29^{lo} population, and the percentage of $\beta 3^+ \text{CD29}^{\text{lo}}$ cells decreased during pregnancy, as previously described (Asselin-Labat et al., 2007) (Figure 2A,B) though some $\beta 3^+$ luminal cells remain (Figure S3A,B). However, to our surprise, we observed increased $\beta 3$ surface levels on the P12.5 CD29^{hi} MaSC-enriched population compared to the virgin gland (Figure 2A,B and S3A,B). Interestingly, this effect is concurrent with the expansion of the CD29^{hi} MaSC pool at this stage (Figure 2A) (Asselin-Labat et al., 2010). This increased $\beta 3$ level was transient, as it decreased to that of virgin glands after full involution (8 weeks) (Figure S3C). The increased $\beta 3$ surface levels in P12.5 CD29^{hi} cells corresponded to a nearly 4-fold induction of $\beta 3$ mRNA compared to virgin CD29^{hi} cells, with little effect on αv levels (Figure 2C), suggesting that this effect is due to enhanced $\beta 3$ expression in these cells. Accordingly, P12.5 $\beta 3^+ \text{CD29}^{\text{hi}}$ cells expressed basal markers (Figure 2D and Figure S3D) consistent with $\beta 3$ co-staining with basal markers in P12.5 mammary sections (Figure S3B). These data show that $\beta 3$ expression is dynamically regulated in CD29^{hi} MaSC/basal cells at mid-pregnancy compared to the virgin gland.

Consistent with $\beta 3$ expression in CD29^{hi} MaSC/basal cells during pregnancy we observed that $\beta 3^+$ epithelial cells ($\text{Lin}^- \text{CD24}^+ \beta 3^+$) from P12.5 mice were unable to form colonies in Matrigel compared to $\beta 3^-$ cells (Figure 2E). However, these same cells from virgin mice were enriched for Matrigel colony-forming cells, in agreement with their characterization as luminal progenitors (Asselin-Labat et al., 2007) (Figure 2E). Thus, in addition to differences in CD29 status, $\beta 3$ expression during pregnancy is associated with a functionally distinct cell population compared to luminal progenitors identified in the virgin mammary gland.

Accordingly, we examined whether $\beta 3^+$ epithelial cells from P12.5 mice were enriched for MaSCs capable of repopulating a fully functional mammary gland similar to CD29^{hi} cells (Asselin-Labat et al., 2010; Shackleton et al., 2006). We tested this possibility by injecting 10,000 $\text{Lin}^- \text{CD24}^+ \beta 3^+$ and $\beta 3^-$ mammary cells from the same donor mice into cleared fat pads of weanling recipients and examining repopulating potential. To simultaneously assess differences in functionality, all outgrowths were harvested at lactating day 2. While few outgrowths were observed in mice injected with $\beta 3^-$ cells (27%), $\beta 3^+$ cells were enriched for repopulating potential (71%) (Figure 2F,G), similar to CD29^{hi} cells (Asselin-Labat et al., 2010; Shackleton et al., 2006). Successful outgrowths all appeared swollen with milk (Figure 2F,H) and the presence of both luminal and basal cell types was validated by immunohistochemistry (Figure 2H). These data show that during pregnancy, epithelial expression of $\beta 3$ is associated with a previously undescribed population of pregnancy-associated MaSCs.

$\beta 3$ is required for expansion of pregnancy-associated MaSCs

During pregnancy, the proportion of CD29^{hi} MaSC/basal cells increases dramatically compared to CD29^{lo} luminal cells (Figure 2A) resulting in an overall increase in MaSC number compared to the virgin gland (Asselin-Labat et al., 2010). Based on the increased $\beta 3$ surface expression we observed in P12.5 CD29^{hi} cells, we considered whether $\beta 3$ is required

for expansion of MaSCs at this stage. We observed that loss of $\beta 3$ from P12.5 CD29^{hi} cells (Figure S4A) decreased the percentage of CD29^{hi} cells relative to CD29^{lo} cells (Figure 3A and Figure S4B). Sorted cell counts showed a similar decrease in the number of CD29^{hi} MaSCs in P12.5 $\beta 3$ KO mice with little or no effect on CD29^{lo} luminal cells (Figure 3B). Interestingly, loss of $\beta 3$ did not affect the number of either cell type in virgin glands, consistent with the absence of a role for $\beta 3$ in luminal progenitors or MaSCs at this stage (Figure 3B). These findings support a specific role for $\beta 3$ in regulating expansion of the MaSC-enriched subset during pregnancy.

This defect in CD29^{hi} cell expansion suggests that $\beta 3$ deletion may result in fewer repopulating cells at mid-pregnancy. To address this we performed limiting dilution mammary gland transplantation assays with CD29^{hi} cells from WT and $\beta 3$ KO P12.5 mammary glands. Results from these experiments showed decreased repopulating frequency in $\beta 3$ KO CD29^{hi} cells (Figure S4C) that corresponded to a 3.6-fold decrease in the absolute number of MaSCs relative to WT mice (Figure 3C). In order to simultaneously test the functionality of these transplants, all outgrowths were harvested on lactating day 2. Interestingly, we noted similar levels of ductal elongation and lobular development in $\beta 3$ KO outgrowths compared to WT (Figure 3D), consistent with the lack of a role for $\beta 3$ in ductal morphogenesis in the adult gland (Figure 1C) or alveolar maturation during late-pregnancy and lactation (Figures S1D,E and S2A). Accordingly, $\beta 3$ deletion failed to affect the number of lobule-limited progenitors present within the CD29^{hi} cell pool (Figure S4D). The more limited outgrowths generated by lobule progenitors are defined by the absence of terminal end bud-like ductal extensions preventing invasion of the fat pad (Bruno and Smith, 2011; Jeselsohn et al., 2010; Smith and Medina, 2008) (Figure S4E). Taken together, these observations highlight a critical role for $\beta 3$ expression in specifically regulating MaSC expansion during mid-pregnancy.

$\beta 3$ signaling is required for MaSC clonogenicity during pregnancy

Decreased MaSC expansion in pregnant $\beta 3$ KO mice suggests a possible defect in MaSC clonogenicity. To evaluate this role for $\beta 3$, we examined mammary cells from virgin or P12.5 WT or $\beta 3$ KO mice for colony formation on irradiated mouse embryonic fibroblasts (MEFs). In order to preserve the luminal-basal crosstalk present in the intact mammary gland we used total mammary cells for these experiments. In this assay MaSC and progenitor cells form colonies that can be distinguished based on morphology (Stingl, 2009) (Figure 4A; top panels) and expression of luminal (E-cadherin) or basal (SMA) markers (Jeselsohn et al., 2010) (Figure 4A; bottom panels). Luminal progenitors form densely-packed colonies that express only E-cadherin, basal progenitors form loose colonies that express only SMA, and MaSCs form mixed colonies that express both E-cadherin and SMA (Jeselsohn et al., 2010; Stingl, 2009).

Examining colony morphology by this method we observed that the proportion of MaSC-like mixed colonies increases at P12.5 (Figure 4A; left panels and Figure 4C) compared to virgin glands (Figure 4B), consistent with the increased frequency of MaSCs observed at P12.5 (Asselin-Labat et al., 2010). Unexpectedly, examination of colonies from WT and $\beta 3$ KO mice showed that $\beta 3$ deletion had no effect on MaSC or luminal colonies in virgin

mice, despite $\beta 3$ acting as a marker of luminal progenitor cells at this stage (Asselin-Labat et al., 2007) (Figure 4B). However, loss of $\beta 3$ significantly decreased the frequency of MaSC and basal colonies at P12.5 compared to WT mice (Figure 4C), with a reciprocal increase in luminal colonies (Figure 4A; right panels and Figure 4C). Importantly, $\beta 3$ deletion did not appear to affect total colony number (Figure 4D). The decreased percentage of MaSC colonies in $\beta 3$ KO mice could alternatively be explained by an increase in luminal progenitors. To directly address this possibility, we performed Matrigel colony formation assays with WT and $\beta 3$ KO CD29^{lo} sorted cells from virgin or P12.5 mice and observed no effect of $\beta 3$ deletion on luminal progenitor cells at either stage (Figure 4E). These data highlight a specific role for $\beta 3$ in regulating MaSC clonogenicity during pregnancy, while having no effect on luminal progenitors in either the virgin or pregnant mammary gland.

In addition to their role as cell adhesion receptors, integrins activate important signaling pathways influencing a diverse array of cell behaviors including proliferation, survival and migration. To examine a role for $\beta 3$ signaling in MaSC/progenitor behavior we analyzed knock-in mice expressing a signaling deficient $\beta 3$ mutant lacking only the last three amino acids of the $\beta 3$ cytoplasmic domain ($\beta 3$ C) (Ablooglu et al., 2009). This mutant prevents the interaction with c-Src and other signaling proteins (Arias-Salgado et al., 2003), resulting in deficient $\beta 3$ signaling, but does not influence ligand binding (Ablooglu et al., 2009; Arias-Salgado et al., 2003; Desgrosellier et al., 2009). Importantly, previous studies showed that cells from $\beta 3$ C knock-in mice express similar levels of $\beta 3$ protein compared to those from WT mice and the $\beta 3$ C mutant forms functional integrin $\alpha v\beta 3$ heterodimers capable of mediating adhesion to $\beta 3$ substrates (Ablooglu et al., 2009), which we validated in P12.5 mammary glands (Figure S5A–D). Similar to the $\beta 3$ KO (Figure 4B,C), no differences were found in colonies from virgin $\beta 3$ C mice (Figure 4F), yet we observed fewer MaSC colonies from $\beta 3$ C mice at P12.5, with proportionally more luminal colonies (Figure 4G). As observed in $\beta 3$ KO mice, total colony number was unchanged upon $\beta 3$ C expression (Figure S5E) and Matrigel assays showed no difference in luminal progenitor cell number (Figure S5F). In fact, examination of P12.5 $\beta 3$ C mammary gland whole-mounts (Figure S5G) and H&E-stained sections (Figure 4H), showed fewer fine branches and alveoli relative to WT mice, similar to the phenotype observed in $\beta 3$ KO mice. These results reveal a role not only for $\beta 3$ expression, but more specifically the $\beta 3$ cytoplasmic signaling domain in contributing to P12.5 MaSC clonogenic activation and mammary gland development during pregnancy.

TGF β 2 stimulates $\beta 3$ expression, enhancing MaSC clonogenicity

While hormones like progesterone have been shown to increase $\beta 3$ expression in MaSC/basal cells of ovariectomized mice (Joshi et al., 2010), this is unlikely to be a direct effect as MaSCs lack steroid hormone receptors (Asselin-Labat et al., 2006). Therefore, to investigate the factors that may account for $\beta 3$ expression in MaSCs during pregnancy, we evaluated several paracrine factors associated with pregnancy such as Transforming Growth Factor β (TGF β) family members and Receptor Activator of NF- κ B Ligand (RANKL). Importantly, both RANKL and TGF β ligands are increased during pregnancy (Asselin-Labat et al., 2010; Fata et al., 2000; Monks, 2007; Robinson et al., 1991), and both pathways affect development of the pregnant mammary gland (Fata et al., 2000; Gorska et al., 2003).

Further, RANKL and TGF β ligands are known to regulate β 3 expression in other systems (Gallier and Schiemann, 2006; Lacey et al., 1998).

To examine the ability of these factors to increase β 3 expression, we stimulated cells from virgin WT mice and measured β 3 expression in MaSC/basal cells, defined by expression of K14 and SMA. Unexpectedly, we found that TGF β 2, but not TGF β 1 or RANKL, stimulated β 3 expression in MaSC/basal cells relative to vehicle-treated cells (Figure 5A). QPCR analysis confirmed TGF β 2's ability to drive β 3 mRNA expression specifically in CD29^{hi} MaSC/basal cells as little effect was observed in CD29^{lo} luminal cells from the same mice (Figure 5B,C). Similar effects were observed in human mammary epithelial cells where TGF β 2 was a potent driver of β 3 expression (Figure 5D). Indeed, we found that TGF β 2 was capable of directly activating the β 3 promoter in these cells as determined using a luciferase reporter plasmid containing the proximal 1300 base pairs of the β 3 promoter upstream of the initial start site (Figure 5E). While TGF β family members commonly induce activation of the SMAD family of transcription factors, analysis of the β 3 promoter failed to identify any SMAD consensus binding elements as assessed by querying the ENCODE whole-genome data in the UCSC genome browser (Raney et al., 2011). However, SMADs commonly exert their transcriptional effects through interacting with SP1 (Feng et al., 2000; Jungert et al., 2006; Poncelet and Schnaper, 2001), which has previously been shown to directly bind the β 3 promoter (Evellin et al., 2013). Accordingly, knock-down of SP1 potently blocked TGF β 2-induced β 3 mRNA and protein expression (Figure 5F,G).

The ability of TGF β 2 to drive β 3 expression suggested that this ligand may affect MaSC clonogenicity in a β 3-dependent manner. Compared to vehicle, only TGF β 2 increased the frequency of bipotent, MaSC-like colonies grown on irradiated MEFs (Figure 5H), with a reciprocal decrease in luminal colonies (Figure 5H), an effect similar to that observed in cells from pregnant mice (Figure 4B,C). This effect was reduced in mammary cells from β 3KO mice (Figure 5H), similar to our results from pregnant β 3KO mice (Figure 4C). TGF β 2 did not affect total colony number unlike TGF β 1, which had a severe growth inhibitory effect, and RANKL which acted as a potent driver of colony formation (Figure 5I). Notably, β 3 did not contribute to colony number in response to any of these factors consistent with results from P12.5 β 3KO mice (Figure 4D). Taken together, these data show that TGF β 2, a critical growth factor released during pregnancy, stimulates β 3 expression in MaSC/basal cells and enhances MaSC clonogenicity in a β 3-dependent manner.

β 3 mediates Slug activation in response to TGF β 2 and pregnancy

The bipotent MaSC-like colonies observed in response to TGF β 2 possess morphological characteristics reminiscent of an epithelial-mesenchymal transformation (EMT) (Figure 5H). This is consistent with a relationship between EMT genes and MaSC/progenitor cell behavior (Guo et al., 2012), particularly during pregnancy (Chakrabarti et al., 2012). Additionally, TGF β family members are well-characterized for their ability to stimulate EMT in development (Moustakas and Heldin, 2007) and cancer (Katsuno et al., 2013). Consistent with this, TGF β 2 stimulation of MCF10A cells drives changes in the expression of EMT markers such as Slug, E-cadherin and Vimentin (Figure S6A). While TGF β 2 induced similar effects on EMT marker protein expression in WT, but not β 3KO 2-D

colonies from virgin mice (Figure S6B,C), no such changes in mRNA expression were noted in sorted CD29^{hi} or CD29^{lo} cells (Figure S6D). Thus, TGF β 2-stimulated changes in colony morphology (Figure 5H) are consistent with increased formation of MaSC-like bipotent colonies, and not an EMT transition of either luminal or basal cells types.

Despite the apparent absence of an effect on EMT, Slug protein levels were consistently reduced in TGF β 2-stimulated β 3KO 2-D colonies compared to WT, specifically in the K14⁺SMA⁺ MaSC/basal cells (Figure S6C). Slug was recently characterized as a determinant of the MaSC fate in the virgin mammary gland (Guo et al., 2012) and is expressed during early to mid-pregnancy, but is negatively regulated by Elf5 during late-stage pregnancy/lactation allowing for alveolar maturation (Chakrabarti et al., 2012). Therefore, we considered whether β 3 was required for TGF β 2-mediated Slug expression in MaSC/basal cells. In virgin WT mammary cells, TGF β 2 induced nuclear Slug expression specifically in K14⁺SMA⁺ cells compared to cells treated with a vehicle control (Figure 6A,B). In contrast, TGF β 2 failed to increase Slug in β 3KO cells (Figure 6A,B) highlighting an essential role for β 3 in TGF β 2-stimulated Slug protein expression in MaSC-enriched basal cells, despite the absence of an effect on Slug mRNA (Figure S6D). Given that TGF β 2 expression is induced during pregnancy (Robinson et al., 1991), we hypothesized that β 3 may similarly regulate Slug expression in the pregnant mammary gland. Compared to WT glands, we observed dramatically reduced levels of nuclear Slug in the K14⁺ basal cells of P12.5 β 3KO mice (Figure 6C,D). Despite this decrease in Slug protein levels, Slug mRNA was unaffected in β 3KO P12.5 CD29^{hi} cells (Figure S6E) similar to the effects observed in TGF β 2-stimulated cells (Figure S6D,F). Thus, β 3 appears to play an integral role in regulating Slug protein expression in MaSC-enriched basal cells in response to TGF β 2 or pregnancy with no effect observed on Slug mRNA.

To determine the potential mechanism by which α v β 3 regulates Slug we considered whether α v β 3 signaling may be required by assessing whether the β 3 β C mutant effects Slug expression. Whereas TGF β 2 induced Slug in K14⁺SMA⁺ mammary cells from virgin WT mice, no increase was observed in cells from β 3 β C knock-in mice (Figure 6E). The β 3 β C mutant has previously been characterized as defective in recruiting and activating Src family kinases (SFKs) (Ablooglu et al., 2009; Arias-Salgado et al., 2003; Desgrosellier et al., 2009). Consistent with this, we noted decreased levels of SFK activation (pY416 SFK) in TGF β 2-stimulated K14⁺SMA⁺ MaSC/basal cells from β 3 β C virgin mice compared to WT cells (Figure S7A) suggesting that α v β 3-mediated SFK activation may be required for Slug expression. Indeed, transient β 3 knock-down in MCF10A cells significantly reduced TGF β 2-induced pY416 SFK and Slug expression (Figure 6F) with no effect observed on Slug mRNA (Figure S6F). Interestingly, treatment with an α v β 3 function-blocking antibody (LM609) failed to effect SFK activation or Slug expression (Figure S7B), suggesting that this role for α v β 3 may be ligand-independent. The absence of an effect on Slug mRNA suggested that α v β 3 may regulate Slug protein through an alternative mechanism. Indeed, Slug protein levels are highly regulated through degradation by the proteasome (Kim et al., 2012; Wu et al., 2012). We found that short-term incubation with a proteasome inhibitor (MG132) was sufficient to restore Slug protein levels to normal in β 3 knock-down cells with little effect on Slug levels in control cells (Figure 6F). Accordingly, short-term incubation with the SFK inhibitor Dasatinib reduced only the TGF β 2-induced Slug protein expression

(Figure 6G). Thus, it appears that TGF β 2-stimulated expression of α v β 3 mediates SFK activation resulting in enhanced Slug protein stability.

α v β 3 is associated with Slug activation and stemness in human breast cancer cells

Previous studies showed that Slug promotes properties associated with both MaSCs and aggressive stem-like breast cancer cells (Guo et al., 2012; Proia et al., 2011). Our observation that α v β 3 regulates Slug in pregnancy-associated MaSCs prompted us to investigate whether a similar relationship exists in human breast cancer cells. Indeed, using gain- and loss-of-function approaches (Figure 7A–C and S7C–F) we found that ectopic expression of β 3 was sufficient to drive Slug nuclear accumulation in both MCF-7 and MDA-MB-468 human breast cancer cells, which lack endogenous β 3 (Figure 7A,C and S7D,F) while β 3 shRNA knock-down in a highly metastatic (HM) variant of the MDA-MB-231 cells (Munoz et al., 2006) reduced nuclear Slug levels compared to control cells expressing a non-silencing shRNA (Figure 7B and S7E). Notably, even unligated α v β 3 was capable of driving Slug expression as assessed with a β 3 mutant deficient in ligand binding (β 3 D119A) (Desgrosellier et al., 2009) (Figure S7C). This is consistent with the inability of α v β 3 antagonists to inhibit Slug expression in non-transformed cells (Figure S7B) and suggests a ligand-independent role for α v β 3. Additionally, the β 3 C mutant was defective in Slug expression compared to full-length β 3 (Figure 7C and S7F) in agreement with our observations from mice (Figure 6E). Thus, β 3 is both necessary and sufficient for Slug activity in human breast cancer cells in addition to regulating Slug expression in pregnancy-associated MaSCs in the mouse.

These findings suggest that α v β 3 may promote stem-like properties in tumor cells which we assessed by tumorsphere formation *in vitro* and limiting dilution tumor initiation experiments *in vivo*. Consistent with the role of unligated α v β 3 in promoting Slug expression, stable β 3 knock-down in triple negative BT-20 and MDA-MB-231 (HM) cells resulted in fewer anchorage-independent tumorspheres relative to controls (Figure 7D and S7E,G). Additionally, β 3 knockdown in MDA-MB-231 (HM) cells reduced the number of tumor-initiating cells compared to control when injected orthotopically into adult female mice at limiting dilution (Figure 7E,F). Importantly, β 3 knock-down had no effect on primary tumor mass in these experiments (Figure 7G), indicating that α v β 3 has a specific effect on tumor-initiating cells and does not affect basic proliferative and survival responses necessary for primary tumor growth, similar to the effects observed in the mammary gland due to β 3 deletion. Together, our findings highlight a conserved role for α v β 3 leading to Slug activity associated with MaSC expansion during pregnancy and stem-like properties in breast cancers.

DISCUSSION

Integrin α v β 3 is found in some of the most aggressive tumor cells in a diverse array of carcinomas including breast cancer, where it is associated with enhanced tumorigenicity and metastasis (Desgrosellier et al., 2009; Felding-Habermann et al., 2001; Liapis et al., 1996; Sloan et al., 2006; Takayama et al., 2005) yet it is unclear if this is related to a role in epithelial stem/progenitor cells. We now show that α v β 3 plays a specific role in driving

MaSC expansion during pregnancy. Genetic deletion of the integrin $\beta 3$ subunit, or expression of a signaling deficient form of this receptor, resulted in defective mammary gland development during pregnancy with no effect on ductal morphogenesis in the virgin gland. This phenotype was associated with increased expression of $\beta 3$ in the MaSC-enriched pool at mid-pregnancy, an effect reproduced by stimulation with TGF β 2 (Figure 7H). Examination of MaSC and progenitor cell activity showed that $\beta 3$ was specifically required for MaSC clonogenicity, expansion and Slug expression during pregnancy with no effect on luminal progenitor cells.

Distinct MaSC/progenitor populations contribute to the development, maintenance and remodeling of the adult mammary gland (Asselin-Labat et al., 2010; Spike et al., 2012; Van Keymeulen et al., 2011; Wagner et al., 2002). MaSC behavior is highly sensitive to steroid hormones released during the estrus cycle and pregnancy (Asselin-Labat et al., 2007; Asselin-Labat et al., 2010; Joshi et al., 2010) and these pregnancy-induced MaSCs possess distinct properties compared to MaSCs in the virgin gland such as more limited self-renewal (Asselin-Labat et al., 2010). Additionally, some MaSC/progenitors are retained post-pregnancy in the parous gland where they represent a functionally distinct population of parity-induced cells (Matulka et al., 2007). We observed that $\beta 3$ levels associated with MaSCs during pregnancy were transient, diminishing to levels found in virgin mice after involution. Thus, $\beta 3$ -expressing MaSCs are unlikely to represent parity-induced cells. Instead, our findings characterize integrin $\alpha v\beta 3$ as a critical determinant of the MaSC state during mid-pregnancy and a requirement for $\alpha v\beta 3$ serves to distinguish these cells from MaSCs required for maintenance in the virgin gland.

To our surprise $\beta 3$ was not required for luminal progenitor cell function despite characterization of $\beta 3$ as a surface marker of luminal progenitor cells in the virgin mammary gland (Asselin-Labat et al., 2007). While our findings show that $\beta 3$ enriches for luminal progenitors in the virgin gland, consistent with others (Asselin-Labat et al., 2007), genetic deletion of $\beta 3$ had no effect on luminal progenitor cell clonogenicity or ductal morphogenesis. This is consistent with other reports where genetic deletion of $\beta 3$ had no effect on ductal morphogenesis in virgin adult murine mammary glands (Taverna et al., 2005). Thus, a potential role for $\alpha v\beta 3$ in tumor cell clonogenicity may be linked to its expression on MaSCs during pregnancy rather than on luminal progenitors.

The steroid hormone progesterone is critical for mammary gland remodeling during pregnancy and regulates $\beta 3$ expression in MaSCs (Joshi et al., 2010). However, MaSCs lack the progesterone receptor (Asselin-Labat et al., 2006), suggesting that progesterone regulates MaSCs indirectly through stimulating release of paracrine factors such as TGF β and RANKL during pregnancy (Asselin-Labat et al., 2010; Fata et al., 2000; Monks, 2007; Robinson et al., 1991). We show that the TGF β family member TGF β 2, and not TGF β 1 or RANKL, drives $\beta 3$ expression in MaSC/basal cells enhancing MaSC clonogenicity. Similar to our observations regarding $\beta 3$ expression and function during pregnancy, progesterone and TGF β family members are critically expressed early in pregnancy (Gorska et al., 2003; Jhappan et al., 1993; Monks, 2007; Robinson et al., 1991) and are reduced in late-pregnancy, allowing lobular maturation (Gorska et al., 2003; Jhappan et al., 1993; Monks, 2007; Robinson et al., 1991). Thus, integrin $\alpha v\beta 3$ may function as a key molecular switch

downstream of progesterone-TGF β signaling that promotes the activation of the MaSC pool during early pregnancy and is reduced in late pregnancy allowing for alveolar secretory maturation.

Pregnancy-associated breast cancers represent some of the most aggressive breast cancers due to frequent metastasis (Schedin, 2006). Interestingly, recent studies have shown that pregnancy is a major regulator of MaSC number and function, suggesting a relationship between MaSCs and pregnancy-associated breast cancers (Asselin-Labat et al., 2010). Accordingly, some proteins that regulate MaSCs during pregnancy also have important functions in aggressive breast tumors (Gonzalez-Suarez et al., 2010; Schramek et al., 2010). Our findings reveal a specific role for integrin $\alpha\beta3$ in regulating Slug expression and MaSC expansion during pregnancy. In breast cancer cells, $\alpha\beta3$ also appears to be necessary and sufficient for Slug activity, anchorage-independent growth, and tumor initiation, properties of stem-like cancer cells (Figure 7H). These findings highlight a potential relationship between $\alpha\beta3$'s function in pregnancy-associated MaSCs and aggressive stem-like breast cancers.

EXPERIMENTAL PROCEDURES

Histological analysis, immunohistochemistry and immunofluorescence

For immunohistochemical staining of formalin-fixed paraffin-embedded tissues, antigen retrieval was performed in citrate buffer at pH 6.0 and 95°C for 20 min. Sections were blocked in normal goat serum diluted in PBS, incubated overnight at 4°C in primary antibody followed by biotin-conjugated anti-rabbit IgG and an avidin–biotin peroxidase detection system with 3,3'-diaminobenzidine substrate (Vector) then counterstained with hematoxylin. Whole-mount mouse mammary glands were fixed in Carnoy's solution and stained with carmine. For quantitation of duct/alveoli density, 3–4 images were randomly sampled from H&E-stained paraffin sections from each mouse with a 4 \times objective and analyzed with Metamorph software. For immunofluorescence, frozen sections or fixed cells were blocked with normal goat serum in PBS and incubated in primary antibody overnight at 4°C followed by secondary at room temperature for 1 h. For further details, see Supplemental Experimental Procedures.

Lysates and immunoblotting

Whole mammary gland lysates were prepared by pulverizing glands flash frozen in liquid nitrogen with a mortar and pestle and then lysing the tissue with RIPA lysis buffer. The lysate was further processed with a hand-held tissue homogenizer and cleared. Whole cell lysates were prepared from cell lines with RIPA lysis buffer combined with scraping. Standard Western blotting procedures were performed. See Supplemental Experimental Procedures for further details.

Flow cytometry and mammary outgrowth assays

Single cell suspensions were prepared and stained with antibodies as described in detail in Supplemental Experimental Procedures. Cell sorting was performed using a FACS Diva or FACS Aria (BD). For outgrowth experiments, sorted cells were injected into the cleared

abdominal fat pads of 3 week old syngeneic recipients. Estimated repopulating cell frequencies were calculated using the ELDA web-based tool (Hu and Smyth, 2009) (<http://bioinf.wehi.edu.au/software/elda/>).

Mammary colony assays

For colony formation on irradiated MEF's, 100,000 MEF's were seeded into 6-well dishes for 48 hr prior to adding 40,000 cells from digested mammary glands and grown in complete DMEM medium. Colonies formed over 5–6 days before fixing and staining with either 0.1% crystal violet/20% methanol/PBS or 2% paraformaldehyde/PBS for immunofluorescent staining and counting colonies.

For Matrigel colonies, 5,000 FACS-sorted mammary gland cells were suspended in 50 μ l growth-factor-reduced Matrigel (BD Pharmingen) and grown 14 days in serum-free Mammary Epithelial Cell Medium-Basal Medium (Cambrex) supplemented with B27 supplement, 20 ng ml⁻¹ epidermal growth factor, 20 ng ml⁻¹ bFGF, 4 μ g ml⁻¹ heparin, 100 units ml⁻¹ penicillin, 100 μ g ml⁻¹ streptomycin. Total colonies per well were counted from each of the 4 replicates per experiment.

Growth factor and inhibitor experiments

Cells from digested mammary glands were seeded at 40,000 cells per well onto MEF's (for colony formation assays) or 8-well chamberslides (Lab-Tek) coated with 2% Matrigel/DMEM. At the time of seeding, cells were suspended in complete DMEM medium supplemented with vehicle (0.1% BSA/PBS), RANKL (50 ng ml⁻¹), TGF β 1 (5 ng ml⁻¹) or TGF β 2 (5 ng ml⁻¹) (Peprotech). Cells were fixed with 2% paraformaldehyde/PBS after 48 h (chamberslides) or 5 days (colonies) for immunofluorescent staining.

For experiments with MCF10A and HMECs, TGF β 2 stimulations were performed with 5 ng ml⁻¹ TGF β 2 (Peprotech) or 0.1% BSA/PBS (vehicle) for 48 h prior to lysis. In some experiments 30 ng ml⁻¹ of the anti- α v β 3 function blocking antibody LM609 (Millipore) was added to cells at the same time as TGF β 2 or vehicle addition. For the proteasome inhibitor experiments, 10 μ M MG132 (Sigma) or DMSO (vehicle) was added to transfected MCF10A cells 5 h prior to lysis. Treatment of MCF10A cells with the Src family kinase inhibitor Dasatinib (Chemietek) or DMSO (vehicle) was performed with 100 nM Dasatinib for the indicated times prior to harvesting lysates.

Orthotopic breast cancer

Tumors were generated by injection of MDA-MB-231 (HM) cells expressing non-silencing or β 3 shRNA at limiting dilution (in 50 μ L sterile PBS) into the inguinal fat pads of adult (12 weeks) female NSG mice. Mice were monitored weekly for tumor formation by gentle palpation. Primary tumor mass was determined by assessing the wet weight of the resected tumors. All tumors formed within 5 weeks, and all tumor-bearing mice were harvested at 6 weeks. Tumor-free mice were harvested at 13 weeks and the absence of any detectable tumor confirmed by whole-mount staining.

Statistical analyses

Data presentation and statistical tests are indicated in the figure legends. For all analyses, $P < 0.05$ was considered statistically significant.

Supplementary Material

Refer to Web version on PubMed Central for supplementary material.

Acknowledgments

We would like to thank Brandon Grosshart and Fernanda Camargo for their technical assistance as well as Hisashi Kato for generously providing lentiviral plasmids containing the $\beta 3$ and $\beta 3$ C cDNAs. We would also like to acknowledge the histology and flow cytometry shared resource facilities at the Moores UCSD Cancer Center. This work was supported by US National Institutes of Health grants CA168692, HL57900 and R3750286 (to D.A.C.) and funding from the California Breast Cancer Research Program grant number 18IB-0020 (to J.S.D.). S.K. was supported by the National Cancer Institute of the National Institutes of Health award number T32CA121938.

References

- Ablooglu AJ, Kang J, Petrich BG, Ginsberg MH, Shattil SJ. Antithrombotic effects of targeting alphaIIb beta3 signaling in platelets. *Blood*. 2009; 113:3585–3592. [PubMed: 19005179]
- Al-Hajj M, Wicha MS, Benito-Hernandez A, Morrison SJ, Clarke MF. Prospective identification of tumorigenic breast cancer cells. *Proc Natl Acad Sci U S A*. 2003; 100:3983–3988. [PubMed: 12629218]
- Arias-Salgado EG, Lizano S, Sarkar S, Brugge JS, Ginsberg MH, Shattil SJ. Src kinase activation by direct interaction with the integrin beta cytoplasmic domain. *Proc Natl Acad Sci U S A*. 2003; 100:13298–13302. [PubMed: 14593208]
- Asselin-Labat ML, Shackleton M, Stingl J, Vaillant F, Forrest NC, Eaves CJ, Visvader JE, Lindeman GJ. Steroid hormone receptor status of mouse mammary stem cells. *J Natl Cancer Inst*. 2006; 98:1011–1014. [PubMed: 16849684]
- Asselin-Labat ML, Sutherland KD, Barker H, Thomas R, Shackleton M, Forrest NC, Hartley L, Robb L, Grosveld FG, van der Wees J, et al. Gata-3 is an essential regulator of mammary-gland morphogenesis and luminal-cell differentiation. *Nat Cell Biol*. 2007; 9:201–209. [PubMed: 17187062]
- Asselin-Labat ML, Vaillant F, Sheridan JM, Pal B, Wu D, Simpson ER, Yasuda H, Smyth GK, Martin TJ, Lindeman GJ, et al. Control of mammary stem cell function by steroid hormone signalling. *Nature*. 2010; 465:798–802. [PubMed: 20383121]
- Bai L, Rohrschneider LR. s-SHIP promoter expression marks activated stem cells in developing mouse mammary tissue. *Genes Dev*. 2010; 24:1882–1892. [PubMed: 20810647]
- Bruno RD, Smith GH. Functional characterization of stem cell activity in the mouse mammary gland. *Stem Cell Rev*. 2011; 7:238–247. [PubMed: 20853073]
- Chakrabarti R, Hwang J, Andres Blanco M, Wei Y, Lukacisin M, Romano RA, Smalley K, Liu S, Yang Q, Ibrahim T, et al. Elf5 inhibits the epithelial-mesenchymal transition in mammary gland development and breast cancer metastasis by transcriptionally repressing Snail2. *Nat Cell Biol*. 2012; 14:1212–1222. [PubMed: 23086238]
- Desgrosellier JS, Barnes LA, Shields DJ, Huang M, Lau SK, Prevost N, Tarin D, Shattil SJ, Cheresch DA. An integrin alpha(v)beta(3)-c-Src oncogenic unit promotes anchorage-independence and tumor progression. *Nat Med*. 2009; 15:1163–1169. [PubMed: 19734908]
- Desgrosellier JS, Cheresch DA. Integrins in cancer: biological implications and therapeutic opportunities. *Nat Rev Cancer*. 2010; 10:9–22. [PubMed: 20029421]
- Evellin S, Galvagni F, Zippo A, Neri F, Orlandini M, Incarnato D, Dettori D, Neubauer S, Kessler H, Wagner EF, et al. FOSL1 controls the assembly of endothelial cells into capillary tubes by direct repression of alpha v and beta 3 integrin transcription. *Molecular and cellular biology*. 2013; 33:1198–1209. [PubMed: 23319049]

- Fata JE, Kong YY, Li J, Sasaki T, Irie-Sasaki J, Moorehead RA, Elliott R, Scully S, Voura EB, Lacey DL, et al. The osteoclast differentiation factor osteoprotegerin-ligand is essential for mammary gland development. *Cell*. 2000; 103:41–50. [PubMed: 11051546]
- Felding-Habermann B, O’Toole TE, Smith JW, Fransvea E, Ruggeri ZM, Ginsberg MH, Hughes PE, Pampori N, Shattil SJ, Saven A, et al. Integrin activation controls metastasis in human breast cancer. *Proc Natl Acad Sci U S A*. 2001; 98:1853–1858. [PubMed: 11172040]
- Feng XH, Lin X, Derynck R. Smad2, Smad3 and Smad4 cooperate with Sp1 to induce p15(Ink4B) transcription in response to TGF-beta. *The EMBO journal*. 2000; 19:5178–5193. [PubMed: 11013220]
- Gallagher AJ, Schiemann WP. Beta3 integrin and Src facilitate transforming growth factor-beta mediated induction of epithelial-mesenchymal transition in mammary epithelial cells. *Breast Cancer Res*. 2006; 8:R42. [PubMed: 16859511]
- Gonzalez-Suarez E, Jacob AP, Jones J, Miller R, Roudier-Meyer MP, Erwert R, Pinkas J, Branstetter D, Dougall WC. RANK ligand mediates progestin-induced mammary epithelial proliferation and carcinogenesis. *Nature*. 2010; 468:103–107. [PubMed: 20881963]
- Gorska AE, Jensen RA, Shyr Y, Aakre ME, Bhowmick NA, Moses HL. Transgenic mice expressing a dominant-negative mutant type II transforming growth factor-beta receptor exhibit impaired mammary development and enhanced mammary tumor formation. *Am J Pathol*. 2003; 163:1539–1549. [PubMed: 14507660]
- Guo W, Keckesova Z, Donaher JL, Shibue T, Tischler V, Reinhardt F, Itzkovitz S, Noske A, Zurrer-Hardi U, Bell G, et al. Slug and Sox9 cooperatively determine the mammary stem cell state. *Cell*. 2012; 148:1015–1028. [PubMed: 22385965]
- Hu Y, Smyth GK. ELDA: extreme limiting dilution analysis for comparing depleted and enriched populations in stem cell and other assays. *J Immunol Methods*. 2009; 347:70–78. [PubMed: 19567251]
- Jeselsohn R, Brown NE, Arendt L, Klebba I, Hu MG, Kuperwasser C, Hinds PW. Cyclin D1 kinase activity is required for the self-renewal of mammary stem and progenitor cells that are targets of MMTV-ErbB2 tumorigenesis. *Cancer Cell*. 2010; 17:65–76. [PubMed: 20129248]
- Jhappan C, Geiser AG, Kordon EC, Bagheri D, Hennighausen L, Roberts AB, Smith GH, Merlino G. Targeting expression of a transforming growth factor beta 1 transgene to the pregnant mammary gland inhibits alveolar development and lactation. *The EMBO journal*. 1993; 12:1835–1845. [PubMed: 8491177]
- Joshi PA, Jackson HW, Beristain AG, Di Grappa MA, Mote PA, Clarke CL, Stingl J, Waterhouse PD, Khokha R. Progesterone induces adult mammary stem cell expansion. *Nature*. 2010; 465:803–807. [PubMed: 20445538]
- Jungert K, Buck A, Buchholz M, Wagner M, Adler G, Gress TM, Ellenrieder V. Smad-Sp1 complexes mediate TGFbeta-induced early transcription of oncogenic Smad7 in pancreatic cancer cells. *Carcinogenesis*. 2006; 27:2392–2401. [PubMed: 16714330]
- Katsuno Y, Lamouille S, Derynck R. TGF-beta signaling and epithelial-mesenchymal transition in cancer progression. *Curr Opin Oncol*. 2013; 25:76–84. [PubMed: 23197193]
- Kim JY, Kim YM, Yang CH, Cho SK, Lee JW, Cho M. Functional regulation of Slug/Snail2 is dependent on GSK-3beta-mediated phosphorylation. *The FEBS journal*. 2012; 279:2929–2939. [PubMed: 22727060]
- Lacey DL, Timms E, Tan HL, Kelley MJ, Dunstan CR, Burgess T, Elliott R, Colombero A, Elliott G, Scully S, et al. Osteoprotegerin ligand is a cytokine that regulates osteoclast differentiation and activation. *Cell*. 1998; 93:165–176. [PubMed: 9568710]
- Liapis H, Flath A, Kitazawa S. Integrin alpha V beta 3 expression by bone-residing breast cancer metastases. *Diagn Mol Pathol*. 1996; 5:127–135. [PubMed: 8727100]
- Lim E, Vaillant F, Wu D, Forrest NC, Pal B, Hart AH, Asselin-Labat ML, Gyorki DE, Ward T, Partanen A, et al. Aberrant luminal progenitors as the candidate target population for basal tumor development in BRCA1 mutation carriers. *Nat Med*. 2009; 15:907–913. [PubMed: 19648928]
- Lim E, Wu D, Pal B, Bouras T, Asselin-Labat ML, Vaillant F, Yagita H, Lindeman GJ, Smyth GK, Visvader JE. Transcriptome analyses of mouse and human mammary cell subpopulations reveal multiple conserved genes and pathways. *Breast Cancer Res*. 2010; 12:R21. [PubMed: 20346151]

- Matulka LA, Triplett AA, Wagner KU. Parity-induced mammary epithelial cells are multipotent and express cell surface markers associated with stem cells. *Dev Biol.* 2007; 303:29–44. [PubMed: 17222404]
- Monks J. TGFbeta as a potential mediator of progesterone action in the mammary gland of pregnancy. *J Mammary Gland Biol Neoplasia.* 2007; 12:249–257. [PubMed: 18027075]
- Moustakas A, Heldin CH. Signaling networks guiding epithelial-mesenchymal transitions during embryogenesis and cancer progression. *Cancer Sci.* 2007; 98:1512–1520. [PubMed: 17645776]
- Munoz R, Man S, Shaked Y, Lee CR, Wong J, Francia G, Kerbel RS. Highly efficacious nontoxic preclinical treatment for advanced metastatic breast cancer using combination oral UFT-cyclophosphamide metronomic chemotherapy. *Cancer Res.* 2006; 66:3386–3391. [PubMed: 16585158]
- Pece S, Tosoni D, Confalonieri S, Mazzarol G, Vecchi M, Ronzoni S, Bernard L, Viale G, Pelicci PG, Di Fiore PP. Biological and molecular heterogeneity of breast cancers correlates with their cancer stem cell content. *Cell.* 2010; 140:62–73. [PubMed: 20074520]
- Poncelet AC, Schnaper HW. Sp1 and Smad proteins cooperate to mediate transforming growth factor-beta 1-induced alpha 2(I) collagen expression in human glomerular mesangial cells. *The Journal of biological chemistry.* 2001; 276:6983–6992. [PubMed: 11114293]
- Proia TA, Keller PJ, Gupta PB, Klebba I, Jones AD, Sedic M, Gilmore H, Tung N, Naber SP, Schnitt S, et al. Genetic predisposition directs breast cancer phenotype by dictating progenitor cell fate. *Cell stem cell.* 2011; 8:149–163. [PubMed: 21295272]
- Raney BJ, Cline MS, Rosenbloom KR, Dreszer TR, Learned K, Barber GP, Meyer LR, Sloan CA, Malladi VS, Roskin KM, et al. ENCODE whole-genome data in the UCSC genome browser (2011 update). *Nucleic acids research.* 2011; 39:D871–875. [PubMed: 21037257]
- Robinson SD, Silberstein GB, Roberts AB, Flanders KC, Daniel CW. Regulated expression and growth inhibitory effects of transforming growth factor-beta isoforms in mouse mammary gland development. *Development.* 1991; 113:867–878. [PubMed: 1821856]
- Schedin P. Pregnancy-associated breast cancer and metastasis. *Nat Rev Cancer.* 2006; 6:281–291. [PubMed: 16557280]
- Schramek D, Leibbrandt A, Sigl V, Kenner L, Pospisilik JA, Lee HJ, Hanada R, Joshi PA, Aliprantis A, Glimcher L, et al. Osteoclast differentiation factor RANKL controls development of progesterin-driven mammary cancer. *Nature.* 2010; 468:98–102. [PubMed: 20881962]
- Shackleton M, Vaillant F, Simpson KJ, Stingl J, Smyth GK, Asselin-Labat ML, Wu L, Lindeman GJ, Visvader JE. Generation of a functional mammary gland from a single stem cell. *Nature.* 2006; 439:84–88. [PubMed: 16397499]
- Sloan EK, Pouliot N, Stanley KL, Chia J, Moseley JM, Hards DK, Anderson RL. Tumor-specific expression of alphavbeta3 integrin promotes spontaneous metastasis of breast cancer to bone. *Breast Cancer Res.* 2006; 8:R20. [PubMed: 16608535]
- Smith GH, Medina D. Re-evaluation of mammary stem cell biology based on in vivo transplantation. *Breast Cancer Res.* 2008; 10:203. [PubMed: 18304381]
- Spike BT, Engle DD, Lin JC, Cheung SK, La J, Wahl GM. A mammary stem cell population identified and characterized in late embryogenesis reveals similarities to human breast cancer. *Cell stem cell.* 2012; 10:183–197. [PubMed: 22305568]
- Stingl J. Detection and analysis of mammary gland stem cells. *J Pathol.* 2009; 217:229–241. [PubMed: 19009588]
- Stingl J, Eirew P, Ricketson I, Shackleton M, Vaillant F, Choi D, Li HI, Eaves CJ. Purification and unique properties of mammary epithelial stem cells. *Nature.* 2006; 439:993–997. [PubMed: 16395311]
- Taddei I, Deugnier MA, Faraldo MM, Petit V, Bouvard D, Medina D, Fassler R, Thiery JP, Glukhova MA. Beta1 integrin deletion from the basal compartment of the mammary epithelium affects stem cells. *Nat Cell Biol.* 2008; 10:716–722. [PubMed: 18469806]
- Takayama S, Ishii S, Ikeda T, Masamura S, Doi M, Kitajima M. The relationship between bone metastasis from human breast cancer and integrin alpha(v)beta3 expression. *Anticancer Res.* 2005; 25:79–83. [PubMed: 15816522]

- Taverna D, Crowley D, Connolly M, Bronson RT, Hynes RO. A direct test of potential roles for beta3 and beta5 integrins in growth and metastasis of murine mammary carcinomas. *Cancer Res.* 2005; 65:10324–10329. [PubMed: 16288021]
- Vaillant F, Asselin-Labat ML, Shackleton M, Forrest NC, Lindeman GJ, Visvader JE. The mammary progenitor marker CD61/beta3 integrin identifies cancer stem cells in mouse models of mammary tumorigenesis. *Cancer Res.* 2008; 68:7711–7717. [PubMed: 18829523]
- van Amerongen R, Bowman AN, Nusse R. Developmental stage and time dictate the fate of Wnt/beta-catenin-responsive stem cells in the mammary gland. *Cell stem cell.* 2012; 11:387–400. [PubMed: 22863533]
- Van Keymeulen A, Rocha AS, Ousset M, Beck B, Bouvencourt G, Rock J, Sharma N, Dekoninck S, Blanpain C. Distinct stem cells contribute to mammary gland development and maintenance. *Nature.* 2011; 479:189–193. [PubMed: 21983963]
- Visvader JE. Keeping abreast of the mammary epithelial hierarchy and breast tumorigenesis. *Genes Dev.* 2009; 23:2563–2577. [PubMed: 19933147]
- Wagner KU, Boulanger CA, Henry MD, Sgagias M, Hennighausen L, Smith GH. An adjunct mammary epithelial cell population in parous females: its role in functional adaptation and tissue renewal. *Development.* 2002; 129:1377–1386. [PubMed: 11880347]
- Wu ZQ, Li XY, Hu CY, Ford M, Kleer CG, Weiss SJ. Canonical Wnt signaling regulates Slug activity and links epithelial-mesenchymal transition with epigenetic Breast Cancer 1, Early Onset (BRCA1) repression. *Proc Natl Acad Sci U S A.* 2012; 109:16654–16659. [PubMed: 23011797]

Highlights

- Pregnancy increases expression of the integrin $\alpha\text{v}\beta\text{3}$ in mammary stem cells (MaSCs)
- $\alpha\text{v}\beta\text{3}$ is critical for initiating alveologenesis and remodeling during pregnancy
- $\alpha\text{v}\beta\text{3}$ mediates pregnancy-induced MaSC expansion, clonogenicity and Slug expression
- In breast cancer, $\alpha\text{v}\beta\text{3}$ similarly regulates Slug expression and stem-like behavior

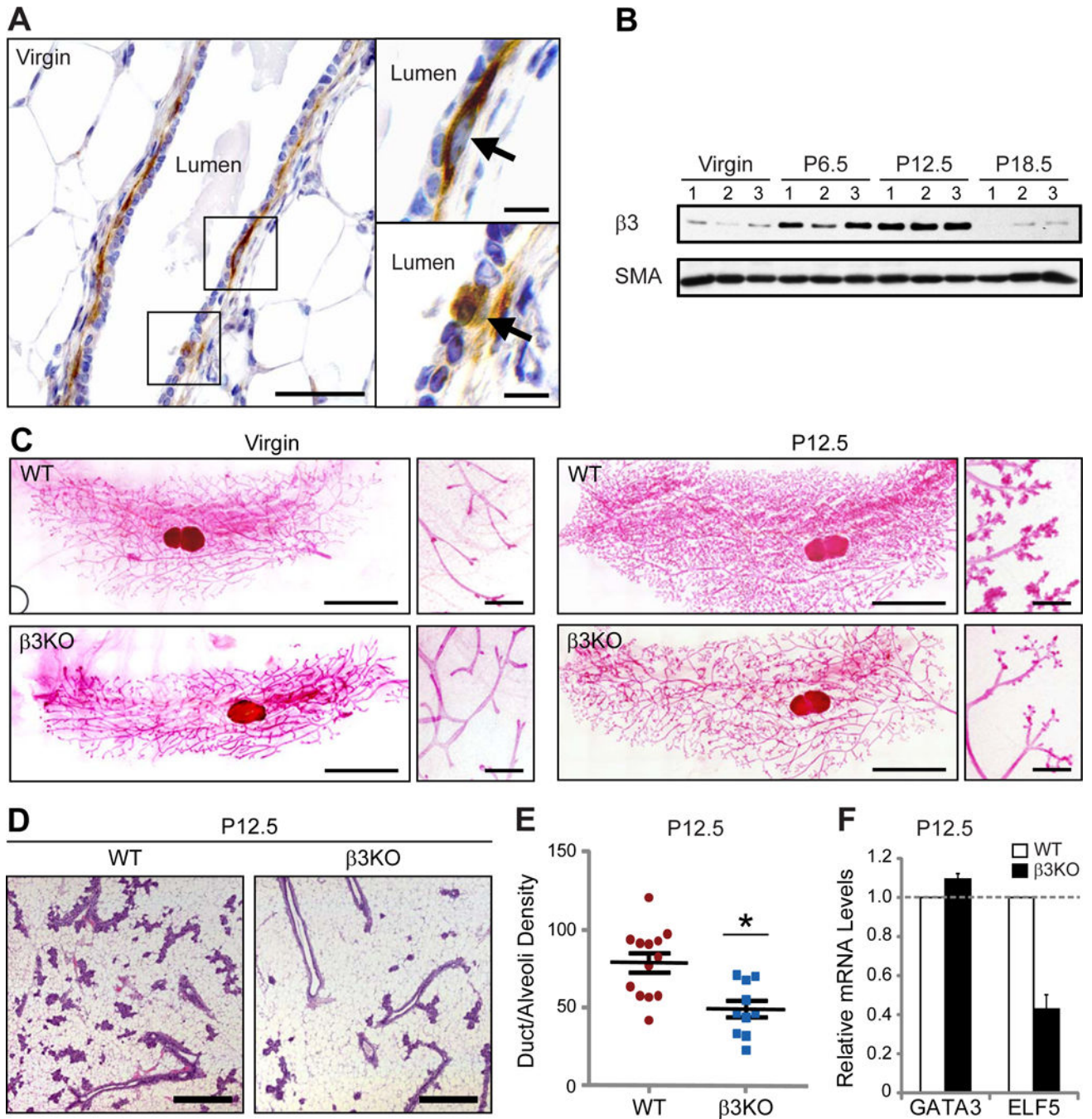


Figure 1. $\beta 3$ is specifically required for mammary gland development during pregnancy
 (A) Representative images of $\beta 3$ immunohistochemistry in an adult virgin murine mammary gland. Shown is an example of a duct (left panel) with areas in boxes shown at high-power (right panels). Images on right show $\beta 3$ -expressing cells (arrows) in the basal epithelial cell layer (top, right) and a subset of luminal epithelial cells (bottom, right). Scale bars, 50 μ m (left panel) and 10 μ m (right panels).
 (B) Western blot of whole mammary gland lysates for $\beta 3$ and α -smooth muscle actin (SMA) (loading control). n=3 mice for each stage.
 (C) Representative images of mammary gland morphology at P12.5 in WT and $\beta 3$ KO mice.
 (D) Representative images of duct/alveoli density at P12.5 in WT and $\beta 3$ KO mice.
 (E) Scatter plot of duct/alveoli density at P12.5 in WT and $\beta 3$ KO mice. * indicates statistical significance.
 (F) Bar graph of relative mRNA levels of GATA3 and ELF5 at P12.5 in WT and $\beta 3$ KO mice.

(C) Mammary gland whole-mounts from virgin and P12.5 WT and β 3KO mice. Virgin; WT, n=8, β 3KO, n=7, P12.5; WT, n=19, β 3KO, n=10. Scale bars, 5 mm (low magnification), and 500 μ m (high magnification).

(D) Representative H&E-stained sections from WT and β 3KO P12.5 mammary glands. Scale bars, 500 μ m.

(E) Quantitation of duct/alveoli density in P12.5 WT versus β 3KO H&E-stained mammary gland sections. WT, n=13, β 3KO, n=10, $P=0.015$. Data shown represent the mean \pm s.e.m. and were analyzed by Student's T-test. $*P<0.05$.

(F) qPCR results displaying the relative amount of GATA3 and ELF5 mRNA in WT and β 3KO P12.5 mammary glands. WT, n=11, β 3KO, n=9. Each sample was run in triplicate and GAPDH was used as a loading control. Data is displayed as the mean \pm s.d. fold change (2^{-CT}) in β 3KO glands relative to WT. See also Figures S1 and S2.

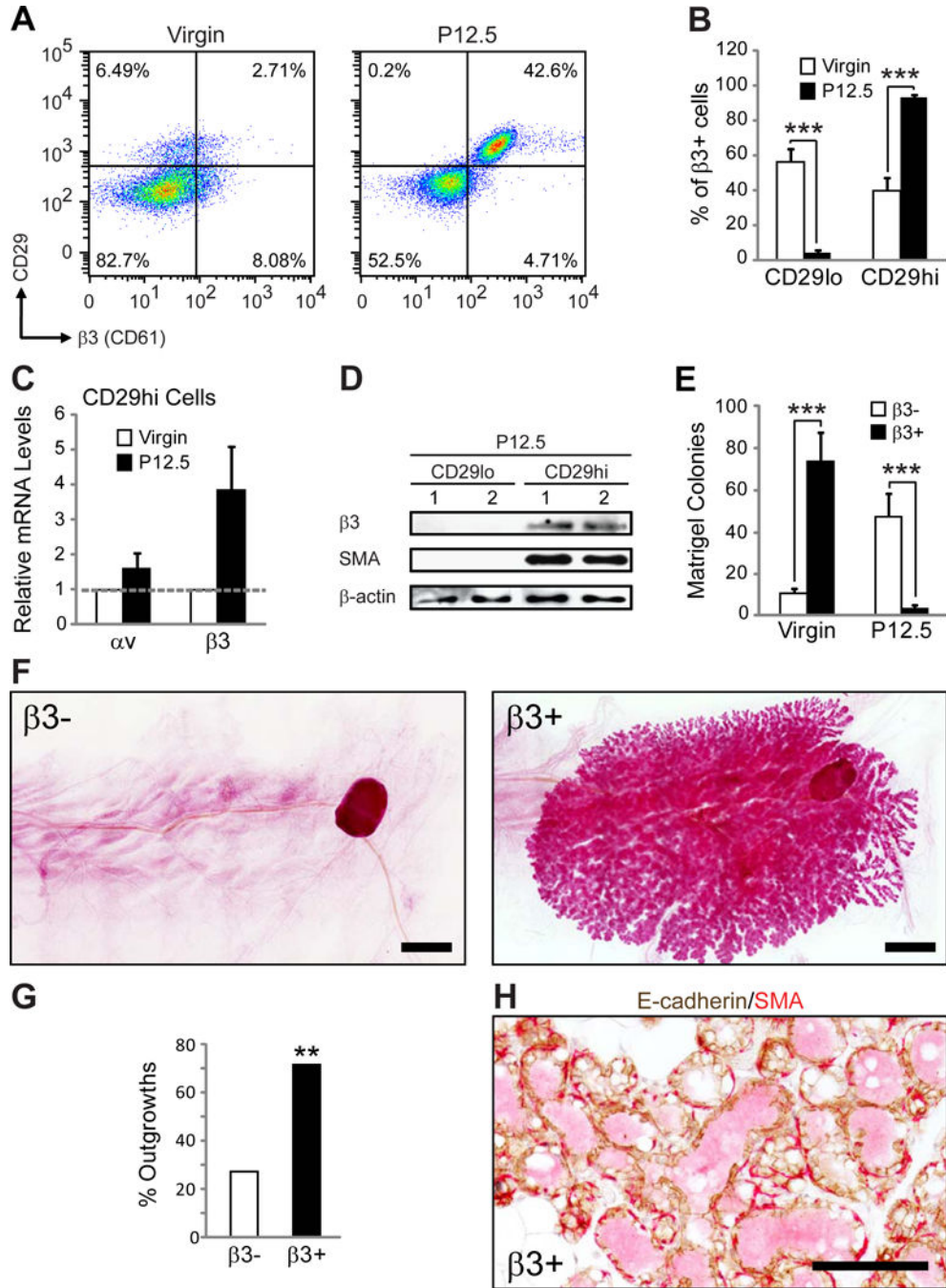


Figure 2. β3 expression is increased in MaSCs during pregnancy

(A,B) FACS analysis of MaSC/progenitor markers in virgin and P12.5 WT mammary glands. (A) Representative FACS density plots showing the live, Lin⁻CD24⁺ cells expressed according to their CD29 (β1 integrin) and β3 status. (B) Histograms showing the percent of Lin⁻CD24⁺β3⁺ cells that are CD29^{lo} or CD29^{hi}. *P*-values for virgin versus P12.5: CD29^{lo}; *P*=0.00014, CD29^{hi}; *P*=0.00008. Data shown are mean ± s.e.m. and were analyzed by Student's *T*-tests. ****P*<0.001. (A,B) Virgin, *n*=8, P12.5, *n*=13.

(C) qPCR data showing the relative levels of αv and $\beta 3$ mRNA in virgin and P12.5 CD29^{hi} cells. Virgin, n=2 (pooled from 2 mice each), P12.5, n=3. Each sample was run in triplicate and 18S rRNA was used as a loading control. Data is displayed as the mean \pm s.e.m. fold change (2^{-CT}) in P12.5 relative to virgin glands.

(D) Immunoblot of FACS-sorted Lin⁻CD24⁺ CD29^{lo} and CD29^{hi} mammary cells from two different P12.5 WT mice for $\beta 3$, SMA (basal marker) and β -actin (loading control).

(E) Matrigel colonies from live Lin⁻CD24⁺ $\beta 3^{+}$ and $\beta 3^{-}$ cells sorted from virgin or P12.5 WT mice. Virgin, n=4, $P=0.00003$, P12.5, n=4, $P=0.0014$. Data represent the mean \pm s.e.m. and were analyzed by paired Student's T-tests. *** $P<0.001$.

(F-H) Mammary gland outgrowth experiments. (F) Representative images of carmine-stained mammary gland outgrowth whole-mounts from P12.5 Lin⁻CD24⁺ $\beta 3^{+}$ and $\beta 3^{-}$ donor cells. Recipients were harvested at lactating day 2. Scale bars, 2 mm. (G) Bar graph showing the frequency of successful mammary gland outgrowths from 10,000 Lin⁻CD24⁺ $\beta 3^{+}$ and $\beta 3^{-}$ donor cells from P12.5 mice. Statistical analysis was performed by Fisher's exact test. $P=0.006$. ** $P<0.01$. (H) Representative image of immunohistochemical staining for E-cadherin (brown) and α SMA (red) in sections from Lin⁻CD24⁺ $\beta 3^{+}$ cell outgrowths. Scale bar, 100 μ m. (F-H) $\beta 3^{-}$, n=22, $\beta 3^{+}$, n=21 mammary glands from 3 independent experiments. See also Figure S3.

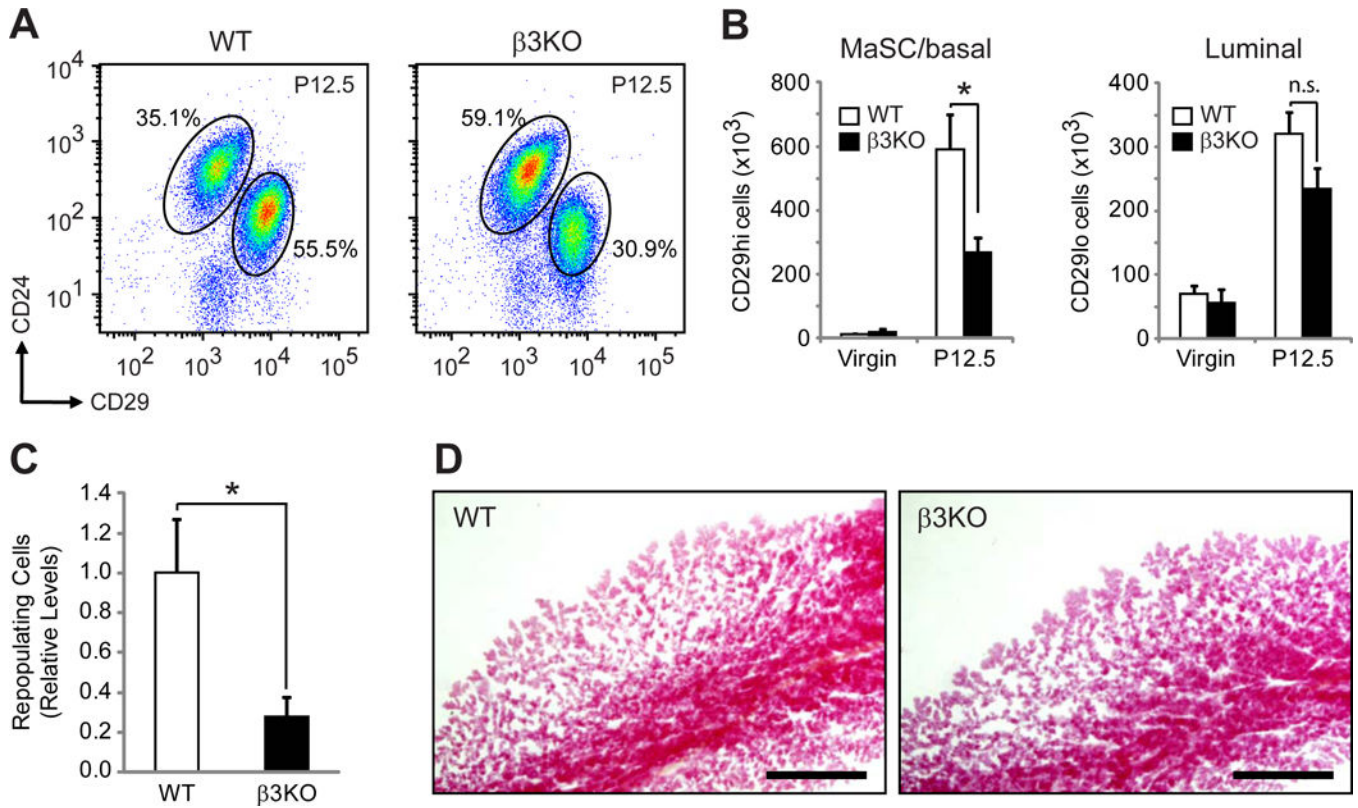


Figure 3. β 3 is required for MaSC expansion during pregnancy

(A,B) FACS analysis of WT and β 3KO virgin and P12.5 mammary glands. (A) Representative FACS density plots of WT and β 3KO P12.5 mammary cells showing the live, Lin⁻ cells expressed according to their CD24 and CD29 status. (B) Quantitation of the total number of FACS-sorted live Lin⁻CD24⁺CD29^{hi} and CD29^{lo} cells from virgin and P12.5 mammary glands. *P*-values for WT versus β 3KO at P12.5: MaSC; *P*=0.027, Luminal; *P*=0.09. (A,B) Virgin; WT, n=4, β 3KO, n=4, P12.5; WT, n=7, β 3KO, n=8.

(C) Histogram showing the relative levels of total repopulating cells in the CD29^{hi} pool from WT and β 3KO P12.5 donor mice. n=4 independent experiments. (B,C) Data represent the mean \pm s.e.m. and statistical analysis was performed by Student's T-tests. **P*<0.05. (B) n.s. = not significant (*P*>0.05).

(D) Representative images of carmine-stained WT and β 3KO outgrowths harvested at lactating day 2. Scale bars, 1 mm. See also Figure S4.

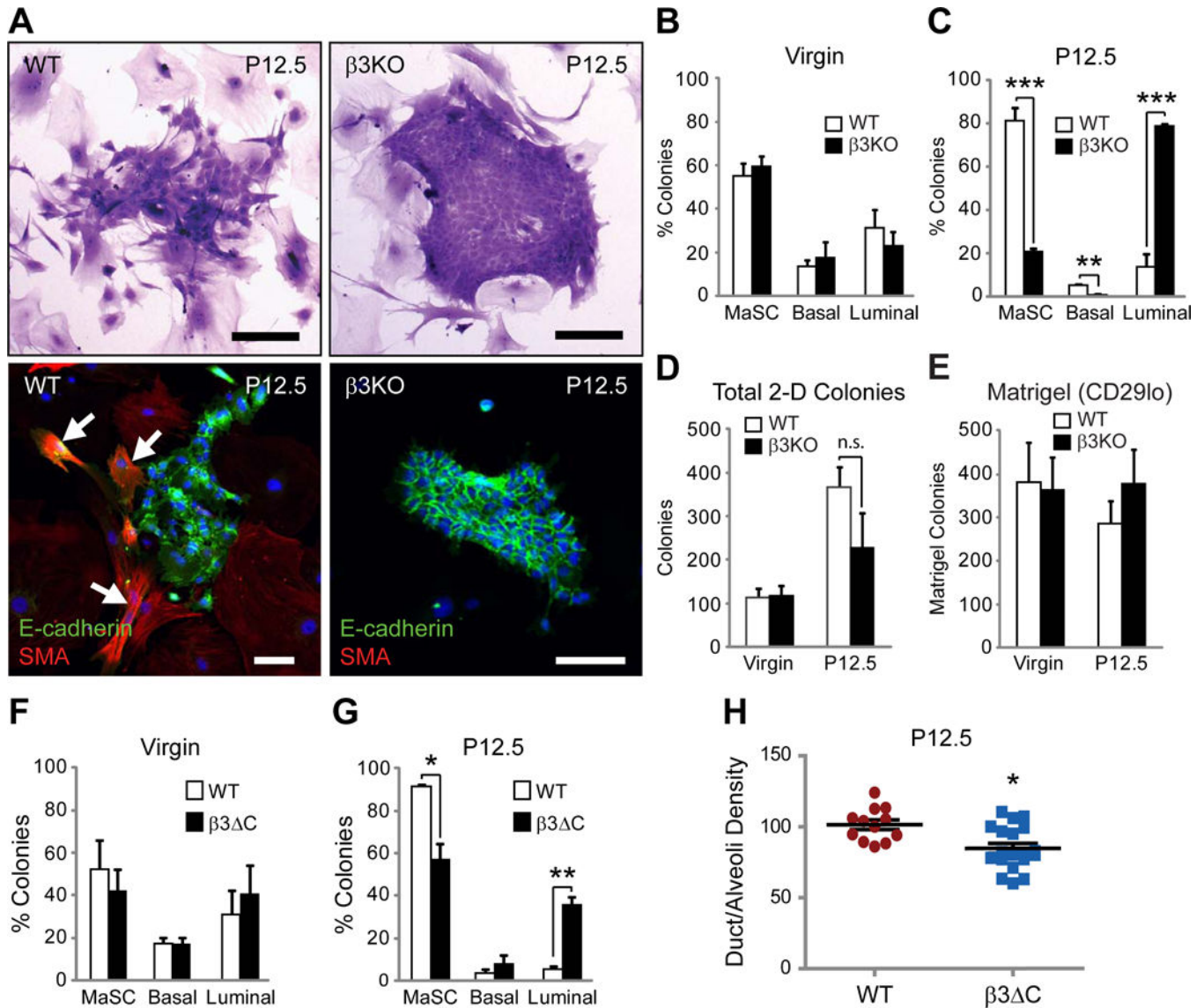


Figure 4. $\beta 3$ signaling is required for pregnancy-associated MaSC colony formation

(A) Representative images of WT and $\beta 3$ KO P12.5 colony morphology on irradiated fibroblasts by crystal violet staining (top panels) or immunofluorescent staining for E-cadherin and SMA (bottom panels). Nuclei are stained blue in all panels. Arrows mark SMA-positive cells. Scale bars, 100 μ m.

(B–D) Quantitation of the percent MaSC, basal, and luminal colonies (B,C) and total colony number (D) from virgin and P12.5 WT and $\beta 3$ KO mice. Virgin; WT, n=6, $\beta 3$ KO, n=6, P12.5; WT, n=5, $\beta 3$ KO, n=4. (C) *P*-values for WT versus $\beta 3$ KO at P12.5: MaSC; *P*=0.0004, Basal; *P*=0.005, Luminal; *P*=0.0004. (D) n.s. = not significant (*P*>0.05).

(E) Histogram depicting colony formation in Matrigel from FACS-sorted CD29^{lo} WT and $\beta 3$ KO cells from virgin and P12.5 mice. Virgin; WT, n=4, $\beta 3$ KO, n=4, P12.5; WT, n=4, $\beta 3$ KO, n=4.

(F,G) MaSC, basal and luminal colonies formed from virgin (F) or P12.5 (G) WT and $\beta 3^{-/-}$ mammary cells grown on irradiated MEF's. Virgin; WT, n=2, $\beta 3^{-/-}$, n=2, P12.5; WT, n=5, $\beta 3^{-/-}$, n=4.

(H) Quantitation of duct/alveoli density in P12.5 WT versus $\beta 3^{-/-}$ H&E-stained mammary gland sections. WT, n=12, $\beta 3^{-/-}$, n=20. (B–H) Data represent the mean \pm s.e.m. and statistical analysis performed by Student's T-tests. * $P < 0.05$, ** $P < 0.01$ *** $P < 0.001$. See also Figure S5.

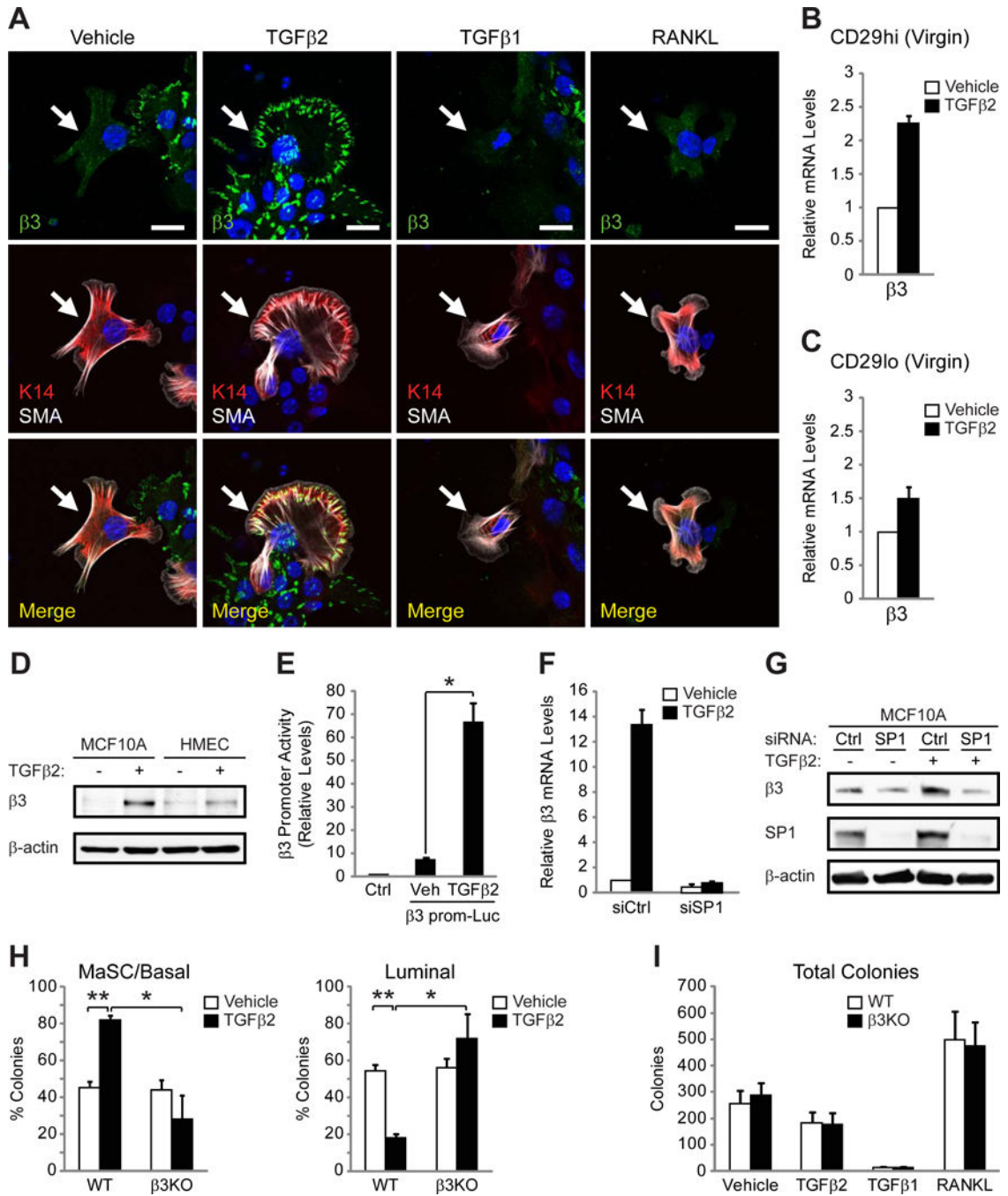


Figure 5. TGFβ2 stimulates β3 expression, enhancing MaSC clonogenicity

(A) Representative immunofluorescent images of β3 expression in K14⁺SMA⁺ cells (arrows) from pooled virgin WT mammary cells stimulated with the indicated growth factors. Nuclei are stained blue in all panels. Scale bars, 20 μm. Data shown are representative of 3 independent experiments.

(B,C) qPCR analysis comparing the relative levels of β3 mRNA in vehicle versus TGFβ2-stimulated CD29^{hi} (B) and CD29^{lo} (C) cells from WT virgin mice. n=2 independent experiments (pooled samples).

(D) Immunoblot for $\beta 3$ and β -actin (loading control) in MCF10As and human mammary epithelial cells (HMECs) stimulated with TGF $\beta 2$ or vehicle control. Data shown is representative of 3 independent experiments.

(E) Histogram displaying the relative luciferase activity in MCF10A cells transfected with an empty vector (Ctrl) or a luciferase reporter plasmid containing the proximal region of the $\beta 3$ promoter ($\beta 3$ prom-Luc) and stimulated with vehicle or TGF $\beta 2$. n=3 independent experiments. $P=0.043$.

(F,G) A representative experiment showing the effect of SP1 knock-down on $\beta 3$ mRNA (F) and protein (G) expression in MCF10A cells stimulated with TGF $\beta 2$ or vehicle control. MCF10A cells transfected with control (siCtrl) or SP1 siRNA (siSP1) were analyzed for $\beta 3$ mRNA expression by qPCR (F) or $\beta 3$ protein by immunoblot (G) in the same experiment. n=3 independent experiments. (B,C,F) Each sample was run in triplicate and 18S rRNA (B,C) or β -actin (F) were used as loading controls. Data is displayed as the mean \pm s.e.m. fold change (2^{-CT}).

(H,I) Quantitation of the percent MaSC/basal, and luminal colonies (H) and total colony number (I) from pooled virgin WT and $\beta 3$ KO mammary cells stimulated with the indicated growth factors. n=3 independent experiments. (H) P -values for vehicle versus TGF $\beta 2$ in WT cells: MaSC; $P=0.0071$, Luminal; $P=0.0071$, and WT versus $\beta 3$ KO cells stimulated with TGF $\beta 2$: MaSC; $P=0.0413$, Luminal; $P=0.0413$. (E,H,I) Data represent the mean \pm s.e.m. and statistical analysis performed by Student's T-tests. * $P<0.05$, ** $P<0.01$.

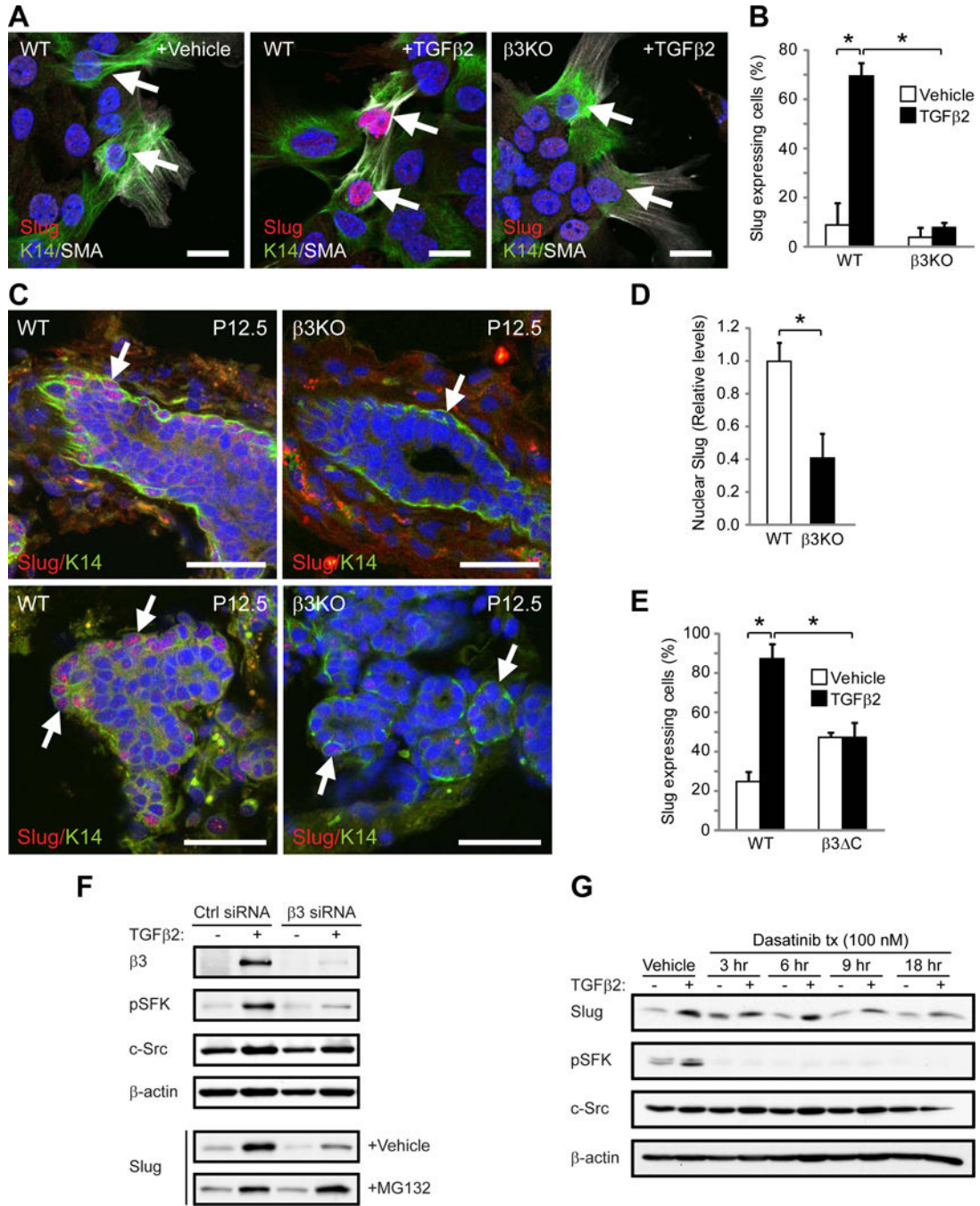


Figure 6. β3 is required for Slug activation in response to TGFβ2 or pregnancy

(A,B) Slug expression in K14⁺SMA⁺ cells from virgin WT and β3KO mammary cells stimulated with vehicle or TGFβ2. (A) Representative images of Slug expression in K14⁺SMA⁺ cells (arrows). Scale bars, 20 μm. (B) Quantitation of the percentage of Slug⁺K14⁺SMA⁺ cells. *P*=0.0439 (vehicle versus TGFβ2 in WT cells) and *P*=0.0342 (WT versus β3KO cells stimulated with TGFβ2). (A,B) WT, *n*=3, β3KO, *n*=3. (C,D) Slug expression in WT and β3KO P12.5 mammary glands. (C) Representative images of Slug in K14⁺ cells (arrows). Scale bars, 20 μm. (A,C) Nuclei are stained blue in all

panels. (D) Histogram showing the relative levels of nuclear Slug expression. Data for each mouse represents the average nuclear Slug expression from 5 fields normalized to total nuclear stain. $P=0.0113$. (C,D) WT, $n=8$, $\beta 3$ KO, $n=6$.

(E) Quantitation of the percentage of Slug-expressing $K14^+SMA^+$ cells from virgin WT and $\beta 3$ C mammary cells stimulated with vehicle or TGF $\beta 2$. WT, $n=2$, $\beta 3$ C, $n=2$. $P=0.029$ (vehicle versus TGF $\beta 2$ in WT cells) and $P=0.032$ (WT versus $\beta 3$ C cells stimulated with TGF $\beta 2$). (B,D,E) Data represent the mean \pm s.e.m. and statistical analysis performed by Student's T-tests. $*P<0.05$.

(F,G) Immunoblots of MCF10A cells stimulated with TGF $\beta 2$ or vehicle control and probed for the indicated proteins. (F) Cells were transfected with Control (Ctrl) or $\beta 3$ siRNA and additionally treated with vehicle or proteasome inhibitor (MG132) for 5 hr prior to lysis. (G) Cells were treated with 100 nM Src inhibitor (Dasatinib) for the indicated length of time prior to lysis. (F,G) Data shown is representative of 3 independent experiments. See also Figures S6 and S7.

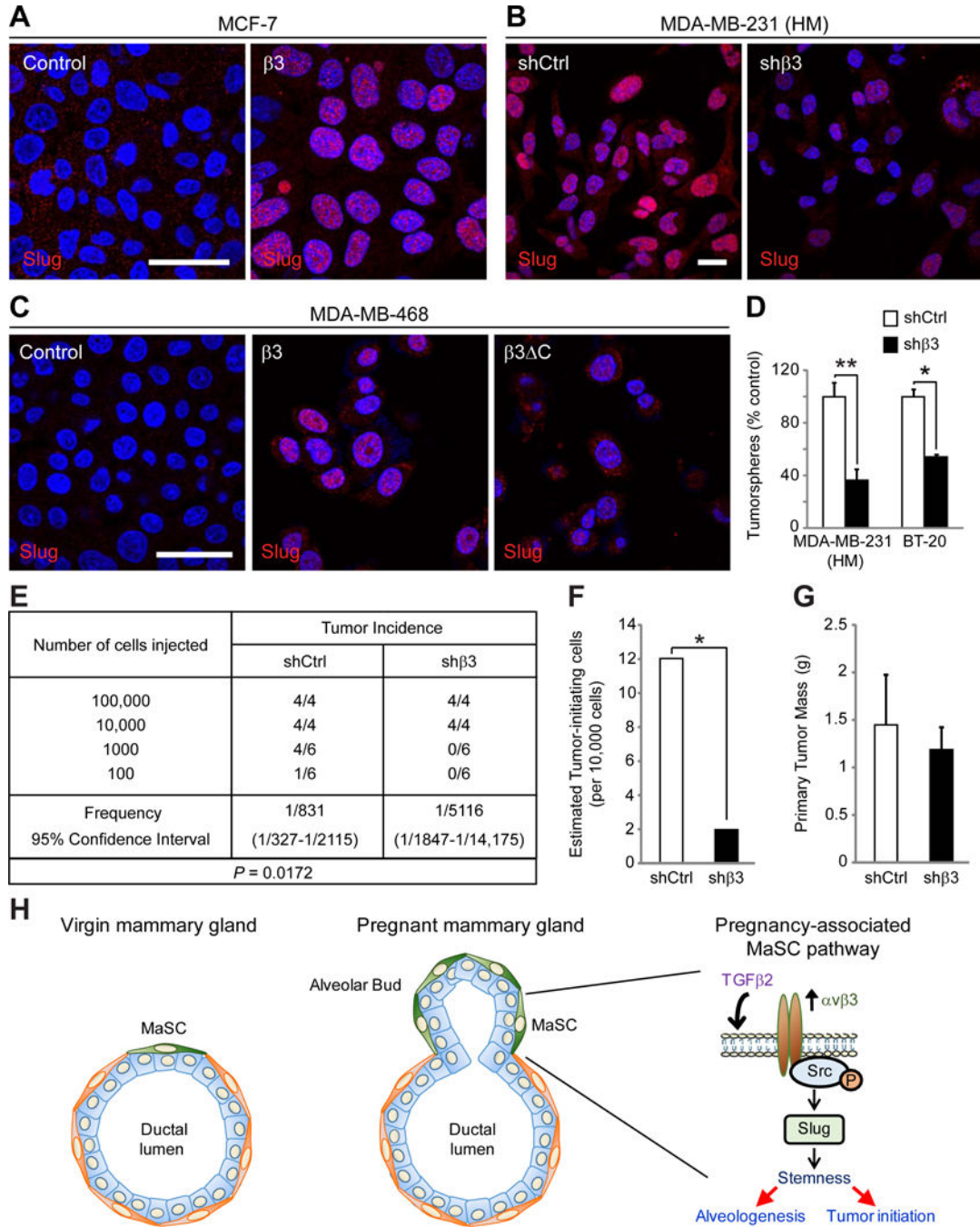


Figure 7. α v β 3 is associated with Slug activation and stemness in human breast cancer cells
(A–C) Representative immunofluorescent images showing Slug expression in (A) MCF-7 cells stably transfected with β 3 cDNA or vector alone (Control) (B) a highly metastatic (HM) variant of MDA-MB-231 cells stably expressing a non-silencing (shCtrl) or β 3 shRNA (sh β 3) and (C) MDA-MB-468 cells stably expressing vector control, full-length β 3 or the β 3 C mutant. (A–C) Nuclei are stained blue in all panels. Scale bars 20 μ m.

(D) Histogram depicting the results of $\beta 3$ knock-down on soft agar colony number in MDA-MB-231 (HM) or BT-20 human tumor cell lines compared to control. MDA-MB-231 (HM), $n=3$, $P=0.0079$, BT-20, $n=2$, $P=0.031$.

(E–G) *In vivo* tumor initiation studies comparing control and $\beta 3$ knock-down MDA-MB-231 (HM) cells injected orthotopically into adult female mice at limiting dilution. (E) Table describing the frequency of tumor formation per fat pad injected for each cell type. (F) Histogram showing the estimated number of tumor-initiating cells from the data in (E). (G) Bar graph depicting the primary tumor mass for each cell type in tumors formed after injection of 10,000 cells and harvested at 6 weeks. (D,G) Data represent the mean \pm s.e.m. and statistical analysis performed by Student's T-test. $*P<0.05$, $**P<0.01$.

(H) Schematic describing the function of the $\alpha v\beta 3$ -Src-Slug signaling axis in MaSC expansion during pregnancy. Compared to the virgin mammary gland (left panel) pregnancy induces expansion of the MaSC population (green cells), resulting in the initiation of alveologenesis (middle panel). Factors released during pregnancy, such as TGF $\beta 2$, drive $\alpha v\beta 3$ expression in these pregnancy-associated MaSCs, resulting in activation of Src family kinases and increased levels of Slug (right panel). This pathway may lead not only to MaSC expansion and alveologenesis during pregnancy, but may additionally contribute to stem-like properties in breast cancer cells, resulting in tumor initiation. See also Figure S7.